Constructive methods for the ground-state energy of fully interacting fermion gases

V. C. Aguilera Navarro,* George A. Baker, Jr., and L. P. Benofy†
Theoretical Division, Los Alamos National Laboratory, University of California, Los Alamos, New Mexico 87545

M. Fortes
Instituto de Física, Universidad Nacional Autónoma de México, Apartado Postal 20-364, 01000 México, Distrito Federal, Mexico

M. de Llano
Department of Physics, North Dakota State University, P.O. Box 5566, Fargo, North Dakota 58105-5566
(Received 18 March 1987)

A perturbation scheme based not on the ideal gas but on a system of purely repulsive cores is applied to a typical fully interacting fermion gas. This is "neutron matter" interacting via (a) the repulsive "Bethe homework-problem" potential, (b) a hard-core–plus–square-well potential, and (c) the Baker-Hind-Kahane modification of the latter, suitable for describing a more accurate two-nucleon potential. Padé extrapolation techniques and generalizations thereof are employed to represent both the density dependence as well as the attractive coupling dependence of the perturbation expansion. Equations of state are constructed and compared with Jastrow–Monte Carlo calculations as well as expectations based on semiempirical mass formulas. Excellent agreement is found with the latter.

I. INTRODUCTION

Since the birth of the quantum many-body problem over fifty years ago, two more or less distinct approaches to understanding the ground-state energy of matter have emerged. One of these approaches is based on perturbation methods;[1] the other, on variational methods.[2] There exist some useful schemes which cannot be readily classified into either of the above two classes, e.g., the $\exp(-S)$ or "coupled-cluster" theory.[3] The variational methods have largely relied on the use of Bijl-Dingle-Jastrow (short-range) correlation functions, while the perturbation methods have been almost entirely based on the ideal (noninteracting) -gas limit of the many-particle system as the unperturbed state. Both have suffered from being eminently low-density theories and as such they are of questionable validity for the description of condensed phases.

It was van der Waals who suggested more than a hundred years ago that the description of fluids could perhaps be tackled best by dividing the pair interactions into repulsive and attractive parts, next developing an accurate description of the fluid of repulsive cores, and finally adding, as small perturbations, the effects of the originally neglected attractions. This remarkable idea has only recently been fully vindicated when (i) it emerged from both classical and quantum-mechanical computer simulations that hard-sphere pair distribution functions are qualitatively similar[4] to those of a *liquid* whose particles interact via a Lennard-Jones potential, and (ii) it was noted[5] that the pair distribution function of an *amorphous solid* (such as Ni-P metallic alloy glass) is remarkably similar to that[6] of a classical system of hard spheres in a random close-packing arrangement. On the other hand, the structure of the ideal gas pair distribution function is drastically different from that of any physical condensed system.

The van der Waals idea has been exhaustively exploited—though not without some difficulty—in constructing[7] what is now considered the most successful theory of classical liquids. It can also be implemented for the quantum-mechanical ground-state problem.[8] One starts with the well-known low-density expansion for the ground-state energy per particle, E/N, for which the first few coefficients have been evaluated with the help of quantum-field-theory diagrammatic techniques[1] and infinite partial summation, among other methods.[9] This expansion is analogous to the well-known Ursell-Mayer virial expansion for the pressure of a classical imperfect gas as a power series in the density, in which the first few so-called "virial" coefficients are known. Unlike the classical virial expansions, however, the quantum-mechanical low-density expansions give rise to *irregular* (i.e., nonpower) series in the density. For example, for either two- or four-species fermion matter composed of N particles, the low-density expansion for the ground-state[10] is

$$\frac{10mE}{3\hbar^2k_F^2N}\equiv\epsilon=1+C_1k_Fa+C_2(k_Fa)^2+[\tfrac{1}{2}C_3r_0/a+C_4A_1(0)/a^3+C_5](k_Fa)^3+C_6(k_Fa)^4\ln|k_Fa| +[\tfrac{1}{2}C_7r_0/a+C_8A_0''(0)/a^3+C_9](k_Fa)^4+o(k_Fa)^4\ . \quad (1)$$

Here m is the mass of each fermion, a the S-wave scattering length, r_0 the S-wave effective range, $A_1(0)$ the P-wave scattering length (cubed), $A_0''(0)$ a second moment of the S-wave scattering length integral,[10] the coefficients C_1 through C_9 pure numbers,[11] and $\hbar k_F$ the Fermi momentum related to the particle density $\rho \equiv N/V$, with V the volume, through

$$\rho = \nu k_F^3/6\pi^2 \quad (\nu = \text{number } of \text{ species}) .$$

For the case of two-species fermion matter $C_6 = 0$. The dynamical quantities a, r_0, and $A_1(0)$ are all pair-potential-shape independent and directly derivable from low-energy phase shifts. They, and also $A_0''(0)$ (which is unrelated to low-energy phase shifts), can be expressed as integrals[12] over the pair potential times the zero-energy scattering radial wave function. They can thus be expanded into the power series

$$f_0 + f_1\lambda + f_2\lambda^2 + \cdots , \tag{2}$$

where λ is an appropriate coupling parameter for the *attractive part* of the pair potential. The coefficients f_i have been determined analytically[11] to sixth order for the hard-core–plus–square-well potential and numerically[13] to 14th order for the Lennard-Jones potential. Substitution of (2) into (1) then leads to the ground-state energy

$$\epsilon(x,\lambda) = \sum_{i=0}^{\infty} \epsilon_i(x)\lambda^i ,$$
$$x \equiv k_F a_0, \quad a_0 \equiv \lim_{\lambda \to 0} a , \tag{3}$$

which is now a *double series* in the density parameter x and the attractive coupling λ. It conforms precisely to the van der Waals idea alluded to above, with $\epsilon_0(x)$ being the low-density expansion for the fluid of repulsive cores, and $\epsilon_i(x)$ $(i = 1,2, \ldots)$ constituting the ith-order perturbative corrections due to the attractions.

In this paper we apply this perturbation scheme to the description of the ground-state energy of neutron matter (hence $\nu = 2$). In Sec. II we use the "Bethe homework-problem" potential;[14,15] in Sec. III we consider hard-core square-well neutrons and evaluate the exact energy per particle in the ladder approximation by numerically integrating the Bethe-Goldstone equation. This energy is then used to deduce the corresponding derivatives in λ with which we construct adequate Padé representations of the first few perturbation terms of the low-density expansion which is correct in the ladder case *only* through k_F^2 in Eq. (1). The ensuing extrapolants are then employed in the reexpanded low-density expansion of the complete theory, correct through the k_F^4 term in Eq. (1), to predict the ground-state energy of the system as a function of density. Section IV contains an application with a more realistic two-neutron potential which permits comparison of the resulting ground-state energies with other calculations as well as with predictions of semiempirical mass formulas. Section V presents our conclusions.

TABLE I. Numerical integration values for the "Bethe homework-problem potential" [Eq. (4)] of two-body scattering parameters appearing in low-density expansion Eq. (1).

a_0(fm)	$A_1(0)$(fm^3)	r_0(fm)	$A_0''(0)$fm^3)
0.689 508 76	0.127 958 55	0.389 293 1	−0.183 756 23

II. "BETHE HOMWORK-PROBLEM POTENTIAL" NEUTRONS

As our first example, we consider an essentially infinite system of neutrons interacting pairwise via the purely repulsive part of the $^1S_0$ Reid[14] soft-core nucleon-nucleon interaction,

$$v_0(r) = 9263.14e^{-4.9r}/r \text{ MeV } (r \text{ in fm}) , \tag{4}$$

also known as the "Bethe homework-problem potential."[15] There is no attraction; $\lambda = 0$ in (2) and (3). The scattering parameters a, r_0, $A_1(0)$, and $A_0''(0)$ are obtainable by numerical integration of Eqs. (3) of Ref. 12, with the results displayed in Table I. We have used the value $\hbar^2/m = 41.555\,99$ MeV fm^2 of Ref. 16 in order to compare with their Jastrow–Monte Carlo calculations. If we take the inverse square root of E and expand about $x \equiv k_F a_0 \to 0$ then the low-density expansion (1) becomes

$$(10mE/3\hbar^2 k_F^2 N)^{-1/2}$$
$$\equiv \epsilon_0^{-1/2}(x) = 1 + F_1 x + F_2 x^2 + F_3 x^3 + F_4 x^4 + \cdots , \tag{5}$$

with the pure number coefficients F_i $(i = 1,2,3, \text{ and } 4)$ known exactly and given in Table II.

In order to extrapolate to nonzero densities, we represent the low-density series (5) by the Padé approximants[17]

$$[L/M](x) = \frac{1 + p_1 x + p_2 x^2 + \cdots + p_L x^L}{1 + q_1 x + q_2 x^2 + \cdots + q_M x^M} \quad (L + M \le 4) , \tag{6}$$

where, by definition, (6) differs from (5) by terms of order x^5 for small x. Figure 1 shows a plot of all fourth-order approximants to the inverse-square-root energy per neutron of the ground state as functions of number density ρ. The ideal Fermi gas equation of state, labeled [0/0] and corresponding to the right-hand side of (5) equal to unity, is shown for comparison. Also shown as open-circled dots are the Jastrow–Monte Carlo (J-MC) results of Ref. 16. These energies, being variational, are upper bounds to the exact energy and are claimed to be only a percent or so above it. Thus on our graph, the open-circled dots are *lower* bounds to the exact result. Of the fourth-order approximants we eliminate all but two: (a) [4/0] corresponds to the truncated low-density polyno-

TABLE II. Coefficients F_i of low-density expansion (5) for "Bethe homework potential" neutrons.

i	1	2	3	4
F_i	−0.176 839	−0.045 860	−0.181 197	+0.132 811

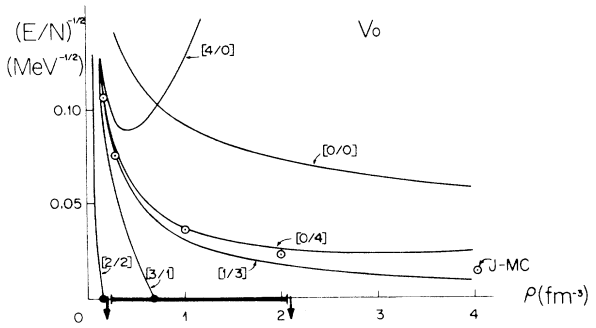

FIG. 1. Inverse square root of energy per particle vs density of the "Bethe homework-problem potential" neutron matter for several Padé approximant $[L/M](x)$ representations of the low-density expression (5). All except the [0/4] and [1/3] extrapolants are discarded for reasons explained in text. Circled dots represent Jastrow–Monte Carlo (J-MC) results from Ref. 16. The horizontal bar on the density axis illustrates spread in theoretical estimates for crystallization density in neutron matter (Ref. 20) while the leftmost arrow mark on the density axis stands for 0.17 fm^{-3} (nuclear saturation density) and the rightmost one for the spinodal point mentioned in the text at 2.1 fm^{-3}. Here $x=k_F a_0$ and $\rho=k_F^3/3\pi^2$, a_0 being the S-wave scattering length from Table I.

mial (5) which is seen to deviate drastically from the J-MC results at all but the lowest densities, (b) [2/2] and [3/1] are discarded since they predict a (second-order) pole in the energy per particle at some finite density value, a situation physically appropriate for *hard-sphere* fermions, as in Ref. 18, but *not* for the soft cores of our interaction (4), which can lead to a (random) close-packing divergence only at infinite density, (c) thus, there only remain the [0/4] and [1/3] extrapolants.

In Table III we compare these results with both the J-MC energies as well as with what is perhaps the next best variational calculation,[19] labeled FHNC/4(JF) (for Fermi hypernetted-chain, with Jackson-Feenberg kinetic-energy form). The [0/4] numbers are somewhat above the J-MC results, and the [1/3] is everywhere somewhat below. Further tests of the accuracy of the present results must of course await Green-function Monte Carlo (GFMC) calculations, which presumably give us exact (nonrelativistic, quantum-mechanical) ground-state energies.

We mention that the [0/4] fails to give a monotonically increasing energy at about 12.6 times nuclear saturation density. This spinodal point (at about $\rho=2.2$ fm^{-3}) is in principle interpretable as an instability of the gaseous phase of the homework neutrons, presumably to a crystalline phase. Other calculations of neutron-matter solidification, reviewed by Canuto,[20] range from about 1.7 to 12 times nucleon saturation (solid horizontal bar in Fig. 1 density axis). The crystalline phrase, if present, has not been treated to our knowledge for this many-body system in either Monte Carlo or FHNC studies. Even though our Padé extrapolations can probably not be relied upon at such high densities, the question of crystallization here appears to remain an open one.

III. HARD-CORE SQUARE-WELL NEUTRONS

We now apply the methods of Ref. 11 to deal with the *attractions* in fermion matter. Specifically, we consider neutrons interacting via the hard-core square-well (HCSW) pair potential

$$v(r)=\begin{cases}+\infty, & 0<r<c\\ -V_0, & c<r<R\\ 0, & r>R\end{cases} \tag{7}$$

and define, as before,[11] the dimensionless range and well-depth parameters

$$\alpha\equiv(R-c)/c,\quad \lambda\equiv mV_0(R-c)^2/\hbar^2\ . \tag{8}$$

As in Refs. 10 and 11, we shall distinguish the "ladder" from the "complete" many-fermion problem. The former corresponds to the summation of so-called ladder, or Brueckner, diagrams to all orders in the interaction, whereas the complete problem includes further diagrams. We recall in Ref. 10 that while the ladder energy reproduces correctly the first *two* coefficients beyond the Fermi kinetic energy term in the low-density expansion, the complete energy reproduces the first *four,* i.e., two more than the ladder.

Although in the *boson* low-density problem the ladder[21] as well as the optimized Jastrow variational scheme[9] both correctly reproduce the first two correction terms in the corresponding low-density expansion about the ideal Bose gas, it has recently been demonstrated[22] that for *fermions* this is not quite accomplished by the Jastrow variational theory, i.e., the second correction coefficient is *not* correctly reproduced within this latter approach.

The main objective of this paper is to construct accurate ground-state energies for neutron matter with attractions, based on the complete low-density expansion

TABLE III. Energy per particle (in MeV) of "Bethe homework-problem potential" neutron matter according to Jastrow–Monte Carlo (J-MC) calculations,[16] Fermi hypernetted-chain variational calculations[19] (FHNC/4) with Jackson-Feenberg (JF) kinetic energy form, and those of the present work (last two columns).

ρ(fm^3)	J-MC	FHNC/4(JF)	$[0/4]^{-2}$	$[1/3]^{-2}$
0.17	89.6±0.7	90	85.93	89.50
0.30	174.9±0.7	177	162.95	167.62
1	782±2	790	703.36	1021.40
2	1976±6	1994	1455.36	3350.89
4	4909±2		1588.04	12 226.94

for two-species fermion matter. Our main strategy will be to develop density Padé extrapolations, and generalizations thereof, within the ladder problem (which is exactly solvable in practice) and then apply these to the complete case to represent, as accurately as possible, the density dependence of the various orders of perturbation corrections, $\epsilon_i(x)$ of Eq. (3), about the hard-sphere fluid. Finally, the perturbation expansion in the attraction is itself represented by the different possible Padé approximants and the convergence to the ground-state energy is studied. In general, fourth-order perturbation theory is found to be more than adequate.

A. Ladder theory

To obtain the ground-state energy per particle E_L/N of fermion matter approximated by the summation of ladder diagrams (with bare kinetic-energy denominator terms), one essentially solves the Bethe-Goldstone integro-differential equation[23] for the perturbed pair wave function, computes with this the matrix elements of the so-called reaction matrix and sums over the occupied states of the Fermi sea. This energy can be calculated[24] to an accuracy within about 0.1%, for any reasonable central potential, with or without a hard core. This was done for the HCSW potentials (7) and (8) for $\alpha=22/7$, $\lambda=2.315\,051$, and several density values in the range $0\le x\equiv k_F c\le 3$. (The upper value corresponds, for neutron matter, to a density of about 84 times nuclear saturation density $\rho_{\rm sat}=0.17$ fm^{-3} for a hard core of diameter $c=0.4F$.) Conversely, nucleon saturation density would correspond, for neutrons, to a value of $x\simeq 0.686$. Table IV summarizes the essentially exact ladder energy shift (from the ideal Fermi gas value).

On the other hand, the low-density expansion for the ladder energy, being of the same form as (1), can be reexpressed, upon substitution of the expansions (2), as

$$\frac{E_L}{N}=\frac{3\hbar^2}{10mc^2}x^2\left\{\epsilon_0(x)+\frac{10}{3}x[\lambda e_1(x)+\lambda^2 e_2(x)+\lambda^3 e_3(x)+\lambda^4 e_4(x)+\cdots]\right\}. \tag{9}$$

TABLE IV. Ladder energy per particle E_L/N for two-species fermions of mass m interacting via a hard-core potential of diameter c surrounded by an attractive square well of range $R=\frac{29}{7}c$ so that $\alpha=(R-c)/c=\frac{22}{7}$ and attractive depth parameter, Eq. (8), $\lambda=2.315\,051$ for several values of $x=k_F c$, as obtained by numerical integration of the Bethe-Goldstone equation.

$x=k_F c$	$\frac{mc^2E_L}{\hbar^2N}-\frac{3}{10}(k_Fc)^2$
0.25	−0.011 293 9
0.50	−0.093 626 7
0.75	−0.343 805
1	−0.763 819
1.5	−1.823 957
2	+18.139 07
3	+74.186 66

We refer to Appendixes A and B of Ref. 11 for details from which the following expressions can be deduced:

$$\begin{aligned}
e_1(x)&=-0.111\,157(1+1.049\,168\,7x+7.236\,696x^2\\
&\quad -1.536\,687x^3+\cdots),\\
e_2(x)&=-0.044\,462(1-0.324\,755x-1.223\,112x^2\\
&\quad -0.200\,440\,5x^3+\cdots),\\
e_3(x)&=-0.017\,996\,6(1-1.666\,323\,2x-5.006\,117x^2\\
&\quad +10.223\,398x^3+\cdots),\\
e_4(x)&=-0.007\,292\,7(1-3.003\,423\,1x-5.879\,447x^2\\
&\quad +26.393\,524x^3+\cdots).
\end{aligned} \tag{10}$$

Note that $e_1(0)/e_2(0)\simeq 2.5$, $e_2(0)/e_3(0)\simeq 2.47$, and $e_3(0)/e_4(0)\simeq 2.47$. In (9) the symbol $\epsilon_0(x)$ stands for the pure hard-sphere term

$$\epsilon_0(x)=10Em/3N\hbar^2k_F^2=1+D_1x+D_2x^2+D_3x^3+D_4x^4+O(x^5), \tag{11}$$

with the coefficients D_i ($i=1,2,3$, and 4) given in Table II of Ref. 11 for both the ladder and complete theories. The Padé representation of (11) found in Ref. 11 is

$$\epsilon_0(x)\hat{=}\{[3/1](x)\}^2=\left[\frac{1+a_1x+a_2x^2+a_3x^3}{1+b_1x}\right]^2, \tag{12}$$

with the coefficients given there, except that the correct values of a_1 and a_3 are 0.249 360 88 and 0.222 171 22, respectively. (The symbol $\hat{=}$ shall stand for "represented by.") Defining for convenience

$$e_0(x)\equiv\frac{3}{10x}[\epsilon_0(x)-1], \tag{13}$$

we show in Fig. 2 the inverse square root $e_0^{-1/2}(x)$ corresponding to the Padé representation (12) compared with the best Padé approximant developed in Refs. 11 and 18 based on the complete low-density expansion. The latter predicts, as it should, a second-order, uncertainty-principle, random close-packing divergence in the energy at some finite density (called the Bernal density ρ_B), marked by a triangle in the figure. By contrast, the ladder Padé representation for the energy does *not* diverge at any finite positive density (since $b_1>0$). This lack of divergence is expected since the exact ladder energy is *finite* for all $k_F<\infty$. Also shown in the figure is the $e_0^{-1/2}(x)$ corresponding to the "exact ladder" energy (dashed curve)

$$e_0(x)=\frac{1}{x}\left[\frac{mE_L}{N\hbar^2k_F^2}-\frac{3}{10}\right]_{\lambda=0}. \tag{14}$$

By differencing the exact E_L/N in λ, we obtained the essentially exact values of $e_i(x)$ ($i=1,2,3$, and 4) defined in Eq. (9) for different values of x. These are given in Table V and are seen to diminish rapidly in magnitude with increasing order. An exhaustive search for adequate fits to this data with Padé approximants to the third-order polynomials of (10), however, yielded *nega-*

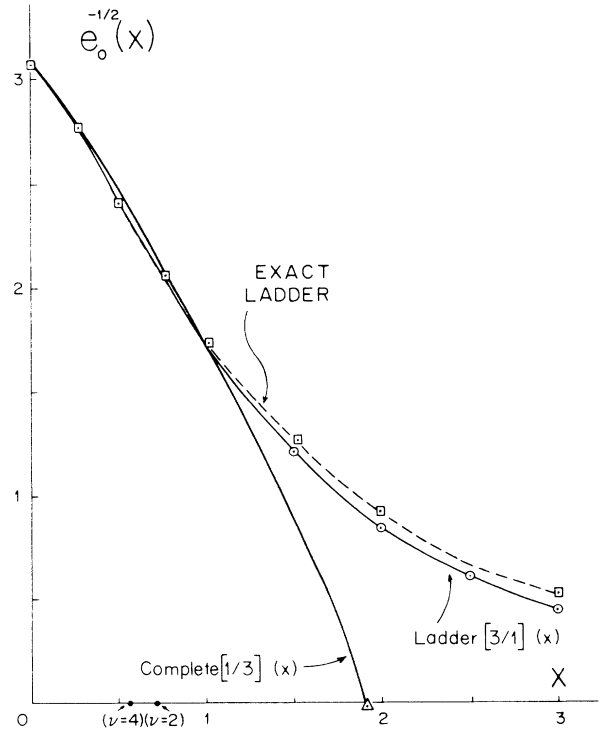

FIG. 2. Inverse square root of Eq. (13), where $\epsilon_0(x)$ is the dimensionless energy per particle Eq. (11) of a two-species fermion fluid of hard spheres of diameter c, vs $x=k_F c$, corresponding to the exact ladder energy Eq. (14) (dashed curve), the $[3/1](x)$ approximant of Ref. 11, Eq. (14), to the low-density ladder energy per particle series as well as the $[1/3](x)$ approximant of Ref. 11, Eq. (18), to the low-density energy series for the complete theory. The triangle on the $x=k_F c$ axis locates the Bernal density for fermion hard spheres (two species) while the two dots on the axis mark the x values corresponding to four- and two-species fermion matter at nuclear saturation density. Note that at these two x values the [1/3] approximant to the complete expansion (5) gives somewhat *lower* energy than the ladder approximation, in either exact (dashed curve) or Padé representation (solid curve) forms. Note also that the latter differs very little from the former for $0\le x\le 1$.

tive results.

To get good fits to $e_i(x)$ two modifications were introduced.

(i) The approximants to the first-order quantity $e_1(x)$ were fixed to yield $-0.476\,018$ when $x=2$, according to Table V, the table of correct ladder values. Since the approximants were forced, from the start, to give e_1 exactly at $x=0$ [see Eq. (10)], they now became *two-point* Padé approximants.[17] The extra condition is equivalent to fixing the coefficient of the x^4 term in the low-density expansion of $e_1(x)$ presented in Eq. (10). Since e_1 is known for several different x, the reader may well wonder why $x=2$ was picked for special consideration. The reason for singling out $x=2$ becomes clear when the complete problem is treated in Sec. III B. The symbol $[L//M](x)$ is now introduced to denote two-point Padé approximants. If

$$e_1(x)=A_1(1+a_1x+a_2x^2+a_3x^3+a_4x^4+\cdots)\,, \tag{15}$$

and $[L//M](x)$ is to correspond to $e_1(x)$, then

$$e_1(x)\hat{=}A_1[L//M](x)\,. \tag{16}$$

(ii) For greater flexibility we utilize what may be called *fractional* Padé approximants. To illustrate what we mean by these approximants consider $e_1(x)$ and raise it to the power n_1, where n_1 is real and positive. Then (15) leads to

$$\begin{aligned} e_1^{n_1}(x)&\simeq A_1^{n_1}(1+a_1x+a_2x^2+a_3x^3+a_4x^4)^{n_1} \quad \text{for } x\ll 1\\ &\simeq A_1^{n_1}(1+\tilde{a}_1x+\tilde{a}_2x^2+\tilde{a}_3x^3+\tilde{a}_4x^4+\cdots)\,, \end{aligned} \tag{17}$$

with

$$\tilde{a}_1\equiv n_1a_1\,, \tag{18}$$

$$\tilde{a}_2=\tfrac{1}{2}n_1(n_1-1)a_1^2+n_1a_2\,, \tag{19}$$

etc. Now determine the two-point Padé approximant corresponding to e_1, namely,

$$e_1^{n_1}(x)\hat{=}A_1^{n_1}[L//M](x)\,. \tag{20}$$

The approximant to $e_1(x)$ given by

$$e_1(x)\hat{=}A_1\{[L//M](x)\}^{1/n_1}\,, \tag{21}$$

is called the *fractional* (in this case, *two-point*) Padé approximant with exponent $1/n_1$.

In trying to fit the accurate values of $e_1(x)$ presented in Table V, we tested fractional approximants with many different exponents. Figure 3 illustrates a typical fit to the ladder data (indicated by open circles). These turned out to be

$$e_1(x)\hat{=}A_1\{[2//2](x)\}^{1/2.4}\,, \tag{22a}$$

$$e_2(x)\hat{=}A_2\{[0/3](x)\}^{1/0.4}\,, \tag{22b}$$

$$e_3(x)\hat{=}A_3\{[0/3](x)\}^{1/0.7}\,, \tag{22c}$$

$$e_4(x)\hat{=}A_4\{[0/3](x)\}^{1/0.375}\,. \tag{22d}$$

Note that only the first-order quantity e_1 is represented by a two-point (fractional) Padé approximant; higher orders are given by standard, or one-point, but fractional, approximants.

Now going back to Eq. (9) for the ladder energy per particle and using (12) for the hard-sphere unperturbed energy term ϵ_0, as well as (22), we arrive at a relation with the form (3). This relation is just a fourth-order polynomial in the coupling constant λ with density-dependent coefficients. We in turn construct all the Padé approximants $[L/M](\lambda)$ of order $L+M\le 4$ to it,

$$\frac{E_L}{N}\hat{=}\frac{3\hbar^2}{10mc^2}x^2[L/M](\lambda)\quad (L+M\le 4)\,. \tag{23}$$

We stress that $[L/M](\lambda)$ is density dependent, that it becomes for $\lambda=0$ the hard-sphere term $[3/1]^2(x)$ of Eq. (12) and that this in turn reduces to unity for $x\to 0$, leaving for Eq. (23) the ideal Fermi gas energy

TABLE V. Essentially exact values of first through fourth derivatives in λ of the ladder energy Eq. (9), obtained by differencing techniques, for several values of $x = k_F c$.

x	$-e_1(x)$	$-e_2(x)$	$-e_3(x)$	$-e_4(x)$
0.25	0.185 384	0.038 169 2	0.008 254 6	0.001 769 3
0.50	0.307 217 9	0.029 192 8	0.003 143 6	0.000 362 3
0.75	0.408 208 2	0.016 954	0.000 934 14	0.000 061
1	0.451 562	0.007 170 4	0.000 170 7	0.000 005 6
1.5	0.490 915	0.002 395 45	0.000 023 8	0.000 000 429
2	0.476 018	0.000 727	0.000 003 81	0.000 000 039 8
3	0.368 20	0.000 172	0.000 000 33	0.000 000 001 56

$3\hbar^2 k_F^2/10m$, as it should.

Figure 4 shows plots of Eq. (23) as a function of density ρ in units of nuclear saturation density $\rho_{sat}=0.17$ fm^{-3}, for the HCSW parameters mentioned before, Eq. (9). Some exact ladder energies deduced from Table IV are also included as open circles. Note the rapid convergence from first, $[1/0](\lambda)$, through fourth, $[4/0](\lambda)$, -order perturbation theory.

The results, as they stand, appear to be extremely reliable to densities considerably beyond ρ_{sat} for this particular two-body interaction. They can still be improved, for example, by reducing the discrepancy (Fig. 2) between the exact ladder $\epsilon_0(x)$ and the adopted Padé approximant by considering both fractional and two-point modifications for the hard-sphere term also. At any rate, even without such improvements our results are sufficiently promising that we proceed to analyze the complete low-density expansion.

B. Complete energy

We now consider the complete low-density expansion for the HCSW potential studied in Sec. III A in the ladder approximation. We take from Appendix B of Ref. 11 the appropriate series expressions for $e_i(x)$, $(i=1,2,3,$ and $4)$. The series are identical in form to Eqs. (10) for the ladder case *except* that the coefficients of all x^2 and x^3 terms will now be *the complete ones* for the ground-state low-density energy expansion. The constant terms plus the coefficients of the x terms will be the same as the ladder ones since, as already mentioned, the ladder approximation correctly reproduces the first *two* corrections to the ideal Fermi gas in the low-density expansion.

For the hard-sphere term $\epsilon_0(x)$ we now take the $[1/3]^2(x)$ representation [Eq. (18) of Ref. 11] of the complete series. This has a second-order (uncertainty principle) pole at $x=x_B=1.939\,15$ corresponding to the (random close-packing) Bernal density $\rho_B=x_B^3/(3\pi^2c^3)=0.1741\rho_0$, where $\rho_0=\sqrt{2}/c^3$ is the regular close-packing density determining a face-centered-cubic arrangement of hard spheres of diameter c. That this predicted value of Fermion ρ_B is reasonable has been discussed in Ref. 18 within the context of random close packing for boson as well as for classical hard spheres.

We use for $e_1(x)$ the two-point, fractional Padé representation found for the ladder case, namely, the

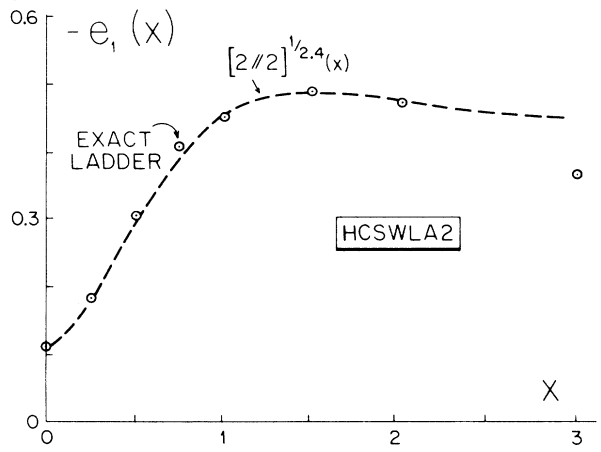

FIG. 3. Plot of fractional, two-point Padé approximant, Eq. (22a), deduced as explained in text, compared to exact ladder energies $e_1(x)$ of Table V (circled dots) for two-species fermion matter interacting via hard-core square-well (HCSW) pair potentials.

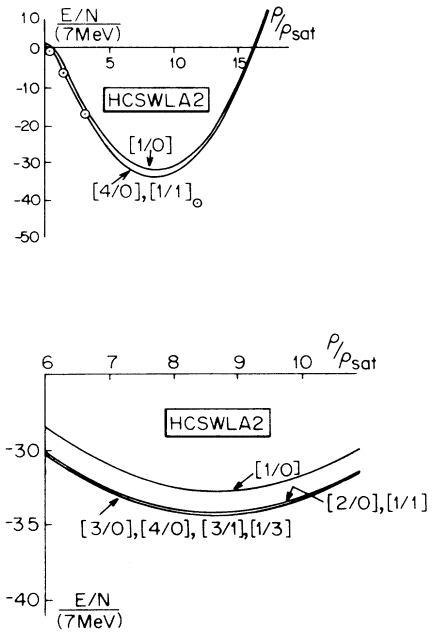

FIG. 4. Ground-state ladder energy (23) deduced from Padé analysis, compared with exact ladder energies of Table IV (circled dots) as function of density in units of nuclear saturation density $\rho_{sat}=0.17$ fm^{-3}. Lower graph is detail of upper graph around the saturation minimum.

$\{[2//2](x)\}^{1/2.4}$, but based, of course, on the coefficients associated with the complete case.

Here the two points of interest for the approximants are $x=0$ and $x=x_B=1.93915$, rather than $x=0$ and $x=2$ as in the ladder case. The following argument shows how the value of $e_1(x)$ at $x=x_B$ can be deduced. The energy per particle has the form

$$\frac{E}{N}=\frac{3}{10}\frac{\hbar^2k_F^2}{m}+\frac{1}{N}\sum_{n=0}^{\infty}E_n\lambda^n\ , \tag{24}$$

with the first-order correction formally given by

$$\lambda E_1=\left\langle\phi\left|\sum_{j=1}^{N}\sum_{\substack{i=1\\(i<j)}}^{N}V(r_{ij})\Theta(r_{ij}-c)\right|\phi\right\rangle\ , \tag{25}$$

where $V(r_{ij})$ is given by Eq. (7) and ϕ refers to the (unspecified) many-body ground-state wave function of the pure hard-sphere reference system. We now argue that near the Bernal density ρ_B we must have

$$\lambda E_1/N=-\tfrac{1}{2}V_0\left[\rho_B\frac{4\pi}{3}R^3-1\right]\quad\text{at }\rho\simeq\rho_B\ . \tag{26}$$

That is to say, the first-order (potential) energy per particle should just be that of the number of sphere centers present within the (spherical) range R of the attractive square well, minus one. Moreover, we expect that the higher-order energies $\lambda E_n/N$ $(n=2,3,\ldots)$ should nearly vanish for $\rho\simeq\rho_B$. By previous definitions the right-hand side of (26) becomes

$$\frac{\hbar^2x^2}{mc^2}\lambda\left[\frac{1.031\,341(\alpha+1)^3-1}{7.520\,605\alpha^2}\right]\ , \tag{27}$$

and thus, for the values of α, c, $\hbar^2/m$, and x_B quoted before,

$$e_1(x_B)=-0.502\,141\,2\ . \tag{28}$$

This is very close to the value $e_1^{\text{ladder}}(2)=-0.476\,018$ of Table V used to construct the ladder, two-point, fractional Padé approximant $\{[2//2](x)\}^{1/2.4}$. We shall instead use (28) for the complete case.

The shapes of the extrapolants (22) corresponding to the complete case turned out to look reasonable except for $e_2(x)=A_2\{[0/3](x)\}^{1/0.4}$ which has a pole around $x\simeq1$, which obviously is very undesirable. In fact, the standard third-order approximant $[0/3](x)$ also has a pole. We thus *augment* our original $\{[0/3](x)\}^{1/0.4}$ extrapolant to the two-point, fractional Padé approximant $\{[2//2](x)\}^{1/0.4}$ with the extra condition $e_2(x_B)=0$. Similarly, the [0/3] approximants for $e_3(x)$ and $e_4(x)$ are likewise augmented, with $e_3(x_B)=e_4(x_B)=0$. The solid curves of Fig. 5 are the results, compared with the ladder (dashed) curves resulting from Eqs. (22). Note that the $e_i(x)$'s obtained with the present procedure mirror the behavior of the *exact* $e_i(x)$'s obtained in Refs. 10 and 11 from a perturbation treatment of coreless, square-well fermions. Namely, $e_1(x)$ *increases* with density but $e_2(x)$, $e_3(x)$, and $e_4(x)$ rapidly *decrease* with density as well as with order for fixed density. This outcome is judged to be of considerable importance.

Finally then, the energy per particle is given (in dimensionless form), for $c=0.4$ fm and $\alpha=22/7$, by

$$\begin{aligned}\frac{E/N}{7\text{ MeV}}=&5.230\,82(\rho/\rho_{\text{sat}})^{2/3}(\{[1/3](x)\}^2-0.370\,523x\{[2//2](x)\}^{1/2.4}\lambda\\&-0.148\,207x\{[2//2](x)\}^{1/0.4}\lambda^2-0.059\,989x\{[2//2](x)\}^{1/0.7}\lambda^3\\&-0.024\,309x\{[2//2](x)\}^{1/0.375}\lambda^4-\cdots)\doteq5.230\,82(\rho/\rho_{\text{sat}})^{2/3}[L/M](\lambda)\\&(L+M\le4)\ ,\end{aligned} \tag{29}$$

where

$$[L/M](\lambda)\underset{\lambda\to0}{\to}\{[1/3](x)\}^2\underset{x\to0}{\to}1\ . \tag{30}$$

In Fig. 6 we display several λ Padé approximants to the complete energy per particle (29) for $\lambda=2.315\,051$ as quoted before. We observed again, rapid convergence, say, from first-order $[1/0](\lambda)$ through fourth-order $[4/0](\lambda)$, (bottom). Note that on the whole, the ladder theory tends to give larger binding, as well as denser saturation, as compared with the complete theory. Neutron matter is of course not expected to be bound—just from the semiempirical mass formula—since the asymmetry energy is positive and larger in magnitude (by about 7 MeV) than the negative volume energy.

We thus turn to an even more realistic HCSW interaction where we shall find the analyses of this section extremely useful.

IV. BAKER-HIND-KAHANE NEUTRONS

A more realistic, but still HCSW, nucleon-nucleon potential is that proposed in Ref. 25. This is the same as the HCSW form considered in Sec. III except that there is *no attractive well* for odd relative angular momentum states to reflect more closely empirical two-nucleon scattering data. It gives $a_{\text{triplet}}=5.39$, $r_{0\,\text{triplet}}=1.71$ fm, $a_{\text{singlet}}=-24$ fm, $r_{0\,\text{singlet}}=2.14$ fm (instead of 2.6 fm), $E_{\text{triplet}}=-2.20$ MeV, and the S-wave phase shift becomes zero at around $E_{\text{lab}}\sim150$ MeV (instead of ~200 MeV). As odd relative angular momentum attractions enter into the low-density expansion for the ground-state energy (1) only via the P-wave scattering quantity $A_1(0)$, i.e., in the k_F^5 term of the energy per particle, and as $A_1(0)$ is expanded (Appendix A of Ref. 11) in powers of $\lambda/(1+\alpha)$, it is sufficient to set equal to zero all terms in

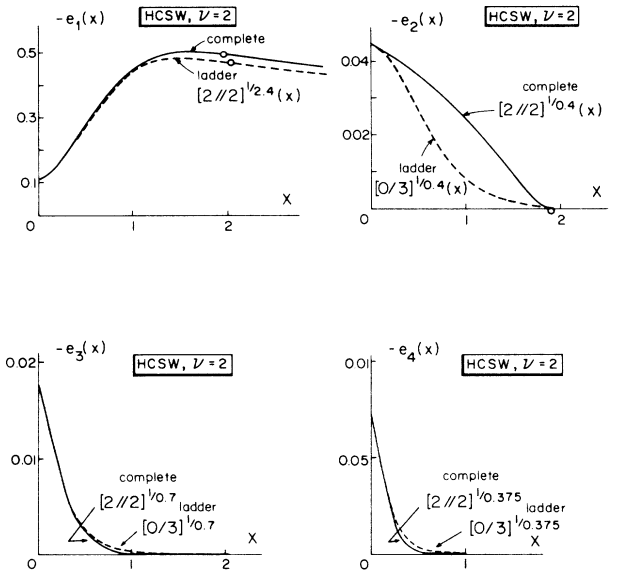

FIG. 5. Comparison between ladder energies and complete energies, extrapolated as explained in text.

the energy expansion (Appendix B of Ref. 11 in $1/(1+\alpha)$ to obtain the corresponding expansion for the BHK potential. The appropriate value of λ is now 2.368 705.

For $e_i(x)$ ($i=1,2,3$, and 4) we first attempted using the forms (22) suggested by the ladder energy study but soon adopted the *two-point,* fractional forms used in the HCSW potential in Eq. (29). These are exemplified for both the ladder (dashed curves) and complete (solid curves) cases, in Fig. 7, and a glance at these shapes suggests the extrapolations to be adequate. The $e_1(x)$ approximant in the complete case develops a pole, Fig. 7 (top), but safely beyond the physical region of densities $0<x<x_B=1.939\,15$.

Substituting the approximants for the complete case of Fig. 7 into Eq. (29), we arrive at the results plotted in Fig. 8 for the energy per particle versus density in units of the nuclear saturation density $\rho_{\rm sat}=0.17$ fm^{-3}. Again, convergence in the perturbation treatment is quite satisfactory, third- and fourth-order approximants practically coinciding. The vertical bar at $\rho=\rho_{\rm sat}$ indicates the spread of values for the energy per particle of neutron matter predicted by various semiempirical mass formulas[26] (where one puts $Z=0$, $N=A\to\infty$, and $e=0$). These date from 1936 to 1971. The approximant labeled $[0/0](\lambda)$ in Fig. 11 refers to the hard-sphere Fermi fluid. The $[2/2](\lambda)$ approximant has not been plotted; it develops a pole at $\rho/\rho_{\rm sat}\simeq 0.2$ and was hence discarded. Our converged results[27] (thick curve) are seen to lie almost at the midpoint of the semiempirical value uncertainty. For comparison, we also display the unpublished variational Monte Carlo (labeled *V-MC*) results[27] using a Jastrow correlation function

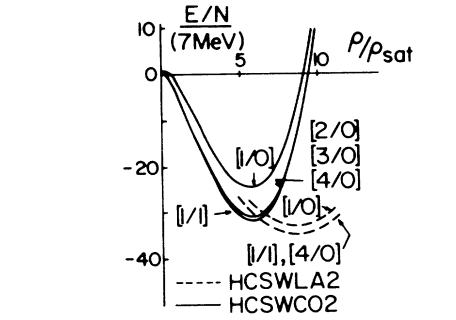

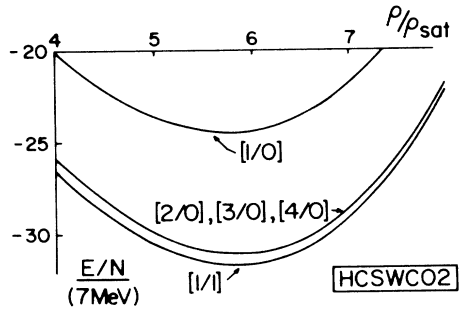

FIG. 6. Same as Fig. 4 but based on the complete low-density expansion, using, however, the fractional Padé extrapolants for $e_i(x)$ complete shown in Fig. 5. Solid curves denote complete results, whereas dashed curves are for ladder results.

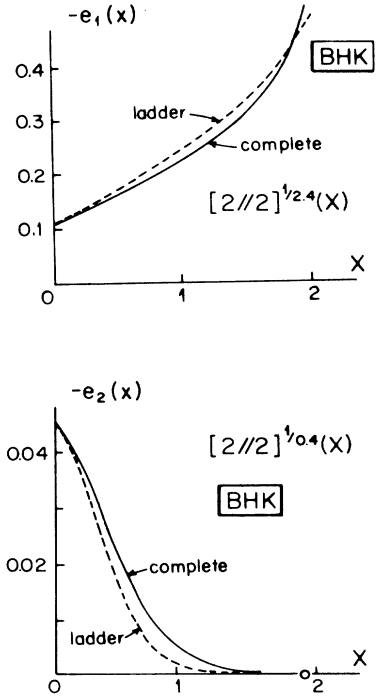

FIG. 7. Comparison of $e_1(x)$ (upper) represented by Eq. (22a) based on the ladder (dashed) and on the complete (solid) low-density expansions, for Baker-Hind-Kahane (BHK) hard-core square-well interacting neutron matter; same for $e_2(x)$ (lower) and Eq. (22b) for ladder and as Eq. (29) for complete low-density expansion. The open circle in the second-order case locates the Bernal density $x_B=1.93915$ where the two-point fractional, density Padé approximants are constrained to vanish in second, third, and fourth order.

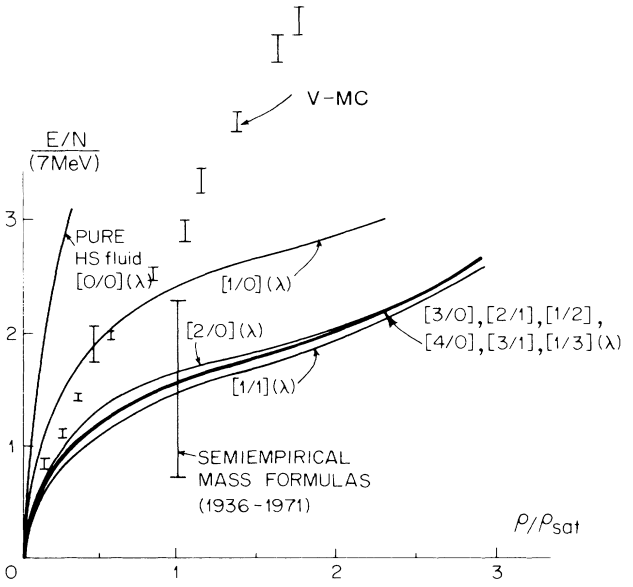

FIG. 8. Complete ground-state energy per particle (in units of 7 MeV) vs density (in units of nuclear saturation density $\rho_{\rm sat}=0.17$ fm^{-3}) for BHK neutron matter as represented by various Padé approximants $[L/M](\lambda)$ in the attractive-well coupling constant $\lambda=2.368\,705$ [see Eq. (29)]. The long vertical bar denotes the spread in semiempirical mass formula values as reported in Ref. 26. The approximant $[0/0](\lambda)$ refers to the hard-sphere fluid without attractions. Finally, the short vertical bars stand for the variational Monte Carlo results of Schmidt.[27]

$$f(r)=\begin{cases}0, & r<c\\ 1-e^{-\mu(r-c)}, & r>c\end{cases} \tag{31}$$

and fixed specific values of μ. They provide a strict *upper* bound to the exact energy. The $[1/1](\lambda)$ approximant emerges as an apparent *lower* bound.

V. CONCLUSIONS

We have illustrated a new perturbation scheme for the ground-state energy of quantum-mechanical fermion fluids which considers as the unperturbed state not the ideal fermion gas but the fermion hard-sphere fluid. The scheme is based on the well-known low-density expansions for the ground-state energy of an interacting many-fermion system, the coefficients of which have been calculated in the literature using the techniques of quantum-mechanical field theory applied to the many-body perturbation scheme which starts from the ideal gas. Our basic tools have been Padé approximants and generalizations thereof, which permit extrapolation to nonzero densities and attractive coupling strengths.

The illustrations refer to neutron mass interacting via (a) the Bethe homework-problem potential, which is purely repulsive, (b) a hard-core–plus–attractive-square-well (HCSW) potential, and (c) the same but with no attraction in states of odd relative angular momentum, i.e., the BHK potential.

For the Bethe homework-problem potential neutrons we find, up to about 24 times nuclear saturation density, energy per particle values everywhere slightly below the presumably best available variational calculation, namely, that of Monte Carlo techniques applied to a Jastrow correlated trial function.

For hard-core–plus–attractive-square-well neutrons we develop our density Padé techniques to fit the exact ladder approximation energies as functions of density. The extrapolants thus derived are applied, with small but crucial changes, to predict the ground-state energy of the so-called complete theory whose low-density expansion contains twice as many correct virial-like coefficients as the ladder theory, namely, four. Finally, the more realistic hard-core square-well two-nucleon BHK potential is employed to construct an equation of state for neutron matter which is compared with the predictions of several semiempirical mass formulas. This comparison is probably to be taken with caution since real neutron mass, being too far away from the "β-stability line," may not be adequately described by semiempirical nucleon mass formulas. However, we include these data for lack of any better, even vaguely suggestive, results for the ground-state energy of neutron matter, save for the variational Monte Carlo results which are an upper bound to the true result for the Hamiltonian treated.

We conclude that the methods used, developed within the context of the exactly soluble ladder problem, might possibly lead to very reliable calculations of the ground-state energy per particle of fermion matter. However, the ultimate test of their reliability will only be had if and when the eagerly awaited results of GFMC computer simulations for interacting many-fermion systems become available.

ACKNOWLEDGMENTS

The authors are grateful to K. E. Schmidt for providing them with variational Monte Carlo results prior to their publication. This work was supported in part by the U.S. Department of Energy. The work of V.C.A.N. was supported in part by Fundação de Amparo e Pesquisa do Estado de São Paulo (FAPESP), Brazil; the work of G.A.B. and L.P.B. was supported in part by U.S. National Science Foundation (NSF) Grant No. INT-84-01865.

*On leave from Instituto de Física Teórica, R. Pamplona 145, São Paulo, Brazil.

†On leave from St. Louis University, St. Louis, MO 63103.

[1]A. L. Fetter and J. D. Walecka, *Quantum Theory of Many-Particle Systems* (McGraw-Hill, New York, 1971).

[2]J. G. Zabolitzky, Adv. Nucl. Phys. **12**, 1 (1981).

[3]H. Kümmel, K. H. Luhrmann, and J. G. Zabolitzky, Phys. Rep. **360**, 1 (1978).

[4]D. A. McQuarrie, *Statistical Mechanics* (Harper and Row, New York, 1976), Chap. 13; M. H. Kalos, D. Levesque, and L. Verlet, Phys. Rev. A **9**, 2178 (1974).

[5]G. S. Cargill III, in *Solid State Physics,* edited by H. Ehrenreich, F. Seitz, and D. Turnbull (Academic, New York, 1975), Vol. 30, p. 227.

[6]J. L. Finney, Proc. R. Soc. London, Ser. A **319**, 479 (1970); **319**, 495 (1970).

[7]J. A. Barker and D. Henderson, Rev. Mod. Phys. **48**, 587 (1976).

[8]G. A. Baker, Jr., M. de Llano, and J. Pineda, Phys. Rev. B **24**, 6304 (1981).

[9]K. Hiroike, Prog. Theor. Phys. **27**, 342 (1962); E. H. Lieb, Phys. Rev. **130**, 2518 (1963).

[10]G. A. Baker, Jr., Rev. Mod. Phys. **43**, 479 (1971).

[11]G. A. Baker, Jr., L. P. Benofy, M. Fortes, M. de Llano, S. M. Peltier, and A. Plastino, Phys. Rev. A **26**, 3575 (1982).

[12]G. Gutiérrez, M. de Llano, and W. C. Stwalley, Phys. Rev. B **29**, 5211 (1984).

[13]E. Buendía, R. Guardiola, and M. de Llano, Phys. Rev. A **30**, 941 (1984).

[14]R. V. Reid, Ann. Phys. (N.Y.) **50**, 411 (1968).

[15]H.-K. Sim Shen and C.-W. Woo, Phys. Rev. D **10**, 3925 (1974); E. Krotscheck and K. Takahashi, Phys. Lett. **61B**, 393 (1976); S. Fantoni and S. Rosati, Nuovo Cimento Lett. **16**, 531 (1976).

[16]D. Ceperley, G. V. Chester, and M. H. Kalos, Phys. Rev. B **16**, 308 (1977).

[17]G. A. Baker, Jr., *Essentials of Padé Approximants* (Academic, New York, 1975); G. A. Baker, Jr. and P. Graves-Morris, in *Encyclopedia of Mathematics and Its Applications,* edited by G.-C. Rota (Addison-Wesley, Reading, Mass., 1981), Vols. 13 and 14.

[18]G. A. Baker, Jr., G. Gutiérrez, and M. de Llano, Ann. Phys. (N.Y.) **153**, 283 (1984).

[19]J. G. Zabolitzky, Phys. Rev. A **16**, 1248 (1977).

[20]V. Canuto, Annu. Rev. Astron. Astrophys. **13**, 335 (1975).

[21]T. D. Lee, K. Huang, and C. N. Yang, Phys. Rev. **106**, 1135 (1957); S. T. Belyaev, Zh. Eksp. Teor. Fiz. **34**, 417 (1958) [Sov. Phys.—JETP **7**, 289 (1958)].

[22]J. C. Owen, in *Recent Progress in Many-Body Theories,* Vol. 142 of *Lecture Notes in Physics,* edited by J. G. Zabolitzky, M. de Llano, M. Fortes, and J. W. Clark (Springer, Berlin, 1981); L. W. Bruch, in Vol. 198 of *Lectures Notes in Physics* (Springer, Berlin, 1984).

[23]H. A. Bethe and J. Goldstone, Proc. R. Soc. London, Ser. A **239**, 551 (1957).

[24]G. A. Baker, Jr., J. L. Gammel, and B. J. Hill, Phys. Rev. **132**, 1373 (1963).

[25]G. A. Baker, Jr., M. F. Hind, and J. Kahane, Phys. Rev. C **2**, 841 (1970).

[26]A. E. S. Green, T. Sawada, and D. S. Saxon, *The Nuclear Independent Particle Model* (Academic, New York, 1968), p. 52; G. Baym, H. A. Bethe, and C. J. Pethick, Nucl. Phys. **A175**, 225 (1971).

[27]K. E. Schmidt (private communication).